Early life stress induces sex-specific changes in behavior and parallel locus coeruleus neuron excitability

Savannah Brannan[1], Ben D Richardson[1]

[1]Department of Pharmacology, Southern Illinois University – School of Medicine, Springfield, IL 62702

Corresponding Author: Ben D Richardson, PhD: brichardson29@siumed.edu

Abstract

Many psychiatric disorders are associated with specific risk factors, including biological sex, chronic stress, and adversity in childhood, but mechanisms underlying these relationships are unknown. The locus coeruleus (LC) is a brain area that contains adrenergic norepinephrine (NE)-releasing neurons with established sex differences in excitability and stress sensitivity. To understand how adversity in early life affects cognitive/affective behavior and LC physiology, we exposed C57BL/6J mice to a dual-phase (early development and adolescence) early life variable stress (ELVS) paradigm and assessed behavior and LC physiology in early adulthood. ELVS caused females, but not males, to display increased novel environment exploration and reduced preference for sucrose. In addition, ELVS caused elevated activity in a familiar environment, modest deficits in Y-maze performance, and altered attention in an operant task, regardless of sex. A reduction in LC neuron excitability, partly due to an increase in action potential delay time, was also found only in female mice exposed to ELVS, paralleling robust behavioral changes. Pharmacological compensation of these changes in LC activity with reboxetine corrected some ELVS-induced behavioral changes. CRF-induced changes in LC neuron activity were also mediated by different preferential signaling pathways in male and female mice, a potential mechanism for lasting sex-specific changes in LC physiology in response to ELVS. Through this animal model of early life stress, we identified sex differences in behavior and parallel changes in LC neuron excitability and CRF sensitivity, identifying mechanisms involved in determining how stress and sex interact to cause LC activity dysregulation and related behavioral changes.

Introduction

Adverse childhood experiences (ACEs) have been shown to increase risk for many neurodevelopmental and affective disorders such as attention deficit hyperactivity disorder (ADHD), autism, anxiety and depression. Although mature neurological systems are often resistant to acute stress, prolonged periods of stress in more malleable and immature systems can alter neurodevelopment [1–5]. The more ACEs a child has, the greater the risk for adverse outcomes. Sex is a biological variable involved in ACEs, leading to adverse psychiatric outcomes, with females showing an increased risk for stress-related disorders in comparison to males [6]. Epidemiological studies indicate women may have increased stress-related disorder development risk/symptom exacerbation during life-phases characterized by hormonal changes that include puberty, menses, pregnancy, postpartum, and menopause [2, 3].

Increased ACE exposures leading to attention, memory, affective, and/or mood disorders represent deficits in behavioral domains is shaped by multiple circuits and modulatory neurotransmitters distributed throughout the central nervous system. For several reasons, we hypothesize that the noradrenergic locus coeruleus system (LC) may be a key neuromodulatory brain area responsible for ACE-related changes in behavior. Optimal activity and processing by multiple circuits to shape multiple behaviors depend upon optimal norepinephrine (NE) release from widely-projecting LC_{NE} neurons (e.g. prefrontal cortex, hippocampus, amygdala, etc. [7–15] to modulate attention [16, 17], cognitive flexibility [18, 19], learned behavior [9, 20], anxiety [10, 21] and reward [10, 14], among others [7]. Specifically, work in animal models indicates that LC-NE neuronal projections to the prefrontal cortex (PFC) and hippocampus are involved in maintaining attention, arousal, and aspects of memory formation [11–13, 22, 23] while those to the amygdala (basolateral and central) shape anxiety and emotional learning behaviors [10, 24, 25], and others modulate sensorimotor integration, associative fear learning, response inhibition, and working memory via projections to the cerebellum [26]. Norepinephrine (NE) release is highly dynamic, as appropriate tonic and phasic [16, 17, 27, 28] activity of LC-NE

60 neurons follow an inverted U-shaped function [7, 29, 30]. As such, low and high NE levels both
61 lead to negative outcomes and behavioral changes in cognitive and affective processes.
62 It is also established that corticotropin-releasing factor (CRF) directly alters the activity of
63 adrenergic neurons in the LC [31–34] and optimal LC neuron activity and related NE release in
64 the prefrontal cortex, amygdala, and hippocampus shape attention, anxiety, and memory [35–39].
65 Animal model data indicate that, compared to males, female LC neurons have different basal
66 physiological properties [40, 41] and elevated CRF sensitivity that can acutely increase basal NE
67 release from LC neurons [42–44]. These types of basal sex differences in CRF-activated signaling
68 may underpin females' increased stress-related disorder prevalence [45, 46]. Despite the
69 established role of NE in cognitive and affective behaviors and sex differences in LC and NE
70 dynamics, how early stress interacts with the sexually-dimorphic LC to shape behaviors
71 associated with LC function (i.e. affect, cognition, and locomotion) is poorly understood. To
72 identify and understand the mechanistic relationship between sex and affective, cognitive, and
73 locomotive behavioral changes associated with stress, we developed a two-phase model of stress
74 exposure early in life to determine how these behaviors are affected and if they are related to sex-
75 specific LC physiology changes. Our results suggest an interaction between sex and stress in
76 affective and cognitive behaviors that involve the LC in C57bl6/J (B6J) mice.

77 **Materials and Methods**

78 *Animals*

79 Male and female C57bl6/J (Jackson Labs, #000664) or Dbh-tdTomato mice (described
80 below) were purchased from Jackson Laboratory and/or bred in-house. To generate mice
81 expressing tdTomato in locus coeruleus noradrenergic neurons under control of dopamine β-
82 hydroxylase (Dbh-tdTomato mice), Dbh-Cre knock-in mice (B6.Cg-*Dbh*$^{tm3.2(cre)Pjen}$*/J*; stock
83 #033951) provided by Patrician Jensen, NIEHS [47] were crossed with homozygous Ai14
84 tdTomato reporter mice (B6.Cg-*Gt(ROSA)26Sor*$^{tm14(CAG-tdTomato)Hze}$/J, Stock #007914) provided by
85 Hongkui Zeng, Allen Institute for Brain Science [48] . All mice were group housed under a reversed

86 12/12-hour light-dark cycle (lights on from 21:00 to 9:00) with *ad libitum* access to food and water.
87 All manipulations and tests were performed during the animals' active dark phase (9:00 to 21:00),
88 unless otherwise stated. All procedures involving animals were conducted in accordance with
89 protocols approved by the Institutional Animal Care and Use Committee (#2022-100) of Southern
90 Illinois University - School of Medicine.

91 *Early Life Variable Stress (ELVS) Animal Model*

92 Male and female C57bl6/J mice were subject to either a two-phase (postnatal and
93 adolescent) early life variable stress (ELVS) paradigm or treated as controls with mice in a litter
94 either exposed to ELVS or treated as controls. The ELVS paradigm consisted of two phases of
95 manipulations, first from postnatal day 6-17 and the second from postnatal day 28-42. First, mice
96 in the ELVS group were isolated together from dams for 4hrs/day during postnatal day 6-10 (P6-
97 10) with access to a warming pad, and then weaned early at postnatal day 17 (P17). Pups were
98 supplemented with nutrient gel (Nutra-gel, Bio-Serv, Flemington, NJ, USA) from P17 to P21.
99 ELVS mice were exposed to sequential variable stressors from P28-42, with each stressor
100 conducted twice on their designated day starting with tape restraint (20 min), forced ice-cold swim
101 in a 40 cm x 10 cm filled container (20 min), 2,3,5-Trimethyl-3-thiazoline (TMT) synthetic fox odor
102 exposure (20 min), light cycle disruption by omission of one night of dark phase, and 48 hours of
103 social isolation. Control male and female C57bl6/J mice were not separated from dams and
104 weaned at P21 and were briefly handled 5 times per week for 10-15 minutes beginning at the
105 same time as the stressors (P28) for the ELVS group.

106 *Behavioral Tests*

107 Behavioral tests were done during the animals' active dark phase in a dimly lit room (~15-
108 20 lux) for testing. Mice were habituated to the testing room for 30 minutes prior to completion of
109 behavioral testing. Mouse performance on all behavioral assays, except for the rotarod, were
110 digitally recorded for analysis. Each apparatus was cleaned thoroughly with scent-free
111 disinfectant between animals.

Open Field Test

Mice were placed in a white acrylic chamber (40 cm x 40 cm wide x 30 cm high square open top chamber) for 30 min with total distance, cumulative time in and number of entrances into center (20 cm x 20 cm) area relative to edges (10 cm border) were analyzed using the EthoVision XT 17 software (Noldus, Wageningen, the Netherlands).

Y-Maze

Mice were placed in a 3-armed “Y” shaped apparatus with symmetrical arms 35 cm in length, 30 cm wall height and 10 cm lane widths at 120-degree angles from one another. Total alternations, or the number of times the mouse enters 3 arms, were recorded and compared to correct (sequential) alternations, where every arm entered within the 3 entrances had not been entered in the immediate previous entrance.

Elevated Zero Maze

Mice were placed in the open arm of an elevated circular platform (50 cm diameter with 5 cm wide track) suspended 61 cm from the floor, with two opposing walled (20 cm high) segments and two open segments in between. The amount of time spent in and entries into the open versus closed segments were calculated using Ethovision XT 17.

Novel Object Recognition and Novel Object Placement Testing

The novel object recognition (NOR) assay was used to assess spatial memory. Following exposure to the open field for 30 min as the chamber acclimation period, the NOR task was performed in the same open field chamber with two phases, each with a 10-minute duration. The first phase was the object habituation period, wherein two identical objects were placed equidistant apart on opposite sides of the chamber. In the second phase, one familiar object from the previous phase was preplaced with a novel object at the same location. Each phase was done on separate days, with the novel object phase occurring 24 h after the same object phase. More time spent with the novel object, was interpreted as increased recall of the familiar object and related to memory and novelty seeking. The amount of time spent with the novel or moved object

138 versus the familiar object is calculated based on the time each mouse spent within 2 cm of the
139 object using Ethovision XT 17. Because this assay was performed in the same arena used as the
140 open field assay, the total distance covered during the second phase (novel object phase) of the
141 assay was also used to determine exploratory activity in a familiar environment to which the
142 mouse had been exposed two previous times.

143 *Sucrose Preference Test*

144 Two weeks before sucrose preference testing (SPT), mice were progressively water-
145 restricted, first to 4 hours of *ad libitum* water access per day for 2 days and then for 2 hours of
146 access per day for 2 days, followed by two days of 24 hr access. This was repeated twice before
147 limiting water access for 22 hrs prior to sucrose preference testing. For SPT, mice were placed in
148 a clean empty cage for one hour with 2 bottles, one bottle containing 1% sucrose solution and a
149 bottle containing water. The sucrose preference index was determined by comparing the amount
150 of sucrose solution versus water consumed by each individual mouse.

151 *Rotarod*

152 Motor and vestibular function was evaluated using the accelerating rotarod (3.17 cm
153 diameter, IITC life Sciences, Inc., Woodland Hills, CA, USA). This rod accelerated in rotations per
154 minute (RPM) from 4 10 40 RPM during the span of 5 minutes. Each mouse received 3 trial
155 sessions per day for two consecutive days for a total of 6 trials. A 10 min rest period was given to
156 the mouse between each trial. The time the mouse fell from the rotating rod onto the platform
157 below was recorded. If the mouse spent a reduced fall time latency, it indicated disrupted motor
158 or vestibular function.

159 *Operant Five-Choice Serial Reaction Time Task (5CSRTT)*

160 For 5SCRTT of attention and learning behaviors, mice were trained using standard
161 5CSRTT protocols (Asinof and Paine, 2014; Humby et al., 2005) and the apparatus was controlled
162 using ABET software (Lafayette Instruments). Two weeks before training, mice will be water
163 restricted starting at 4 hours of ad libitum access per day, reducing to 2 hours per day. During

164 training sessions, the mice were given sweetened condensed milk as a reward for correctly
165 performing the task and weighed to ensure they were at the proper weight after water restriction.
166 The operant conditioning chamber (30.5 x 24.1 x 29.2 cm) consisted of 2 Plexiglas sidewalls, an
167 aluminum front wall and back wall, and a stainless-steel grid floor will be used to carry out this
168 experiment (Lafayette Instruments). The front wall contained five nose poke apertures (2.5 x 2.2
169 x 2.2 cm each) with each aperture containing a light-emitting diode (LED) and an infrared sensor
170 cable to detect mouse nose insertions. The mice were trained by progressively shortening the
171 intertrial interval and stimulus duration for 30 minutes daily for 5-7 days per week to reach baseline
172 performance with intertrial interval (ITI) of 5sec and the stimulus duration of 0.8sec. Once mice
173 reached the criterion threshold of 80% correct trials with <30% of trials omitted, they were
174 assessed again on ten different variations with either shorter or longer ITI, shorter or longer
175 stimulus duration, aperture light brightness, sound and light distractor manipulations, and
176 combinations of these changes relative to the standard variables used during training. Response
177 accuracy (% correct) and response omissions (# of premature responses during ITI) for each
178 variable condition, along with the number of premature responses during specific training stages,
179 were evaluated for differences based on mouse sex and treatment as control or exposure to
180 ELVS.

181 *Reboxetine Administration*

182 In a separate cohort of 7-9-week-old control and ELVS mice, 2 mg/kg reboxetine diluted
183 into apple juice or apple juice alone (100 µl) was given to control and ELVS C57bl6/J mice one
184 hour prior to behavioral testing on SPT, open field, and y-maze. To determine reboxetine effects
185 on these behaviors, one behavior was evaluated each day on consecutive days with pre-test
186 apple juice/reboxetine administered each day 1 hr prior to each assay. The order of the behavioral
187 assays was kept the same for all mice.

188 *Ex vivo Acute Brian Slice Preparation*

189 Animals were anesthetized with 4% isoflurane, followed by intracardial perfusion with ice-
190 cold oxygenated N-Methyl-D-glucamine (NMDG) artificial cerebrospinal fluid (NMDG-ACSF),
191 which contained (in mM): 92 NMDG, 2.5 KCl, 0.5 $CaCl_2$, 10 $MgCl_2$, 1.2 NaH_2PO_4, 30 $NaHCO_3$, 20
192 HEPES, 25 D-glucose, 2 ascorbic acid, 2 thiourea, and 3 sodium pyruvate and had an osmolarity
193 of 300–310 mOsm with pH adjusted to 7.3–7.4 with HCl. Coronal slices (250 μm thick) that
194 included the LC were sectioned in ice-cold NMDG-ACSF using a Compresstome vibrating
195 microtome (Processionary Instruments, LLC) and were transferred to a holding chamber
196 containing NMDG-ACSF at 35 °C where the NaCl concentration increased steadily over 25 min.
197 After 30 min, slices were transferred to a modified HEPES-based ACSF (HEPES-ACSF, 35 °C),
198 which contained (in mM): 92 NaCl, 2.5 KCl, 2 $CaCl_2$, 2 $MgCl_2$, 1.2 NaH_2PO_4, 30 $NaHCO_3$, 20
199 HEPES, 25 D-glucose, 2 ascorbic acid, 2 thiourea, 3 sodium pyruvate, and 3 myo-inositol and
200 had an osmolarity of 300–310 mOsm with pH 7.3–7.4. After incubating slices in HEPES-ACSF at
201 35 °C for 1 hr, slices were maintained in HEPES-ACSF at room temperature until being
202 transferred to the recording chamber where they were continuously perfused at a 3-5 ml/min with
203 oxygenated ACSF, which contained (in mM): 125 NaCl, 2.5 KCl, 2 $CaCl_2$, 2 $MgCl_2$, 1NaH_2PO_4,
204 26 $NaHCO_3$, 20 D-glucose, 2 ascorbic acid, and 3 myo-inositol and had an osmolarity of 310–320
205 mOsm with pH 7.3–7.4.

206 *Ex vivo Acute Brain Slice Whole-Cell Electrophysiology*

207 Neurons in the LC were visualized using an upright microscope (Olympus BX51WI) with
208 a 40x water-immersion objective. The microscope was able to detect interference contrast and
209 imaged via an infrared-sensitive camera connected to a video monitor. Whole-cell patch-clamp
210 recordings were performed at 32 °C maintained with an in-line solution heater from visually
211 identified LC neurons using the 4th ventricle as a landmark. Noradrenergic neurons in the LC were
212 identified by the presence of tdTomato in Dbh-tdTomato mice and action potential properties of
213 putative noradrenergic LC neurons in C57bl6/J mice were verified to be similar to Dbh-tdTomato+
214 neurons.

215 Using a horizontal puller (P1000, Sutter Instruments, Novato, CA, USA), patch pipettes
216 were pulled from filamented borosilicate glass capillaries (outer diameter 1.5 mm, inner diameter
217 0.86, Sutter Instruments), having a tip resistance of 5–7 MΩ when filled with potassium gluconate-
218 based internal solution that contained (in mM): 139.6 mM K-gluconate, 0.4 mM KCl, 4 mM NaCl,
219 0.5 mM $CaCl_2$, 10 mM Hepes, 5 mM EGTA free acid, 4 mM Mg-ATP, 0.5 mM Na-GTP with an
220 osmolality 285–290 mOsm and the pH adjusted to 7.2-7.3 with KOH (E_{Cl} = -85 mV). The
221 calculated liquid junction potential of 15.5 mV was left uncorrected. For experiments assessing
222 the role of ATP-sensitive potassium channels, all nucleotide salts were removed from the internal
223 solution. For voltage-clamp recordings of synaptic activity, 5 mM QX-314 was included in the
224 internal solution (iso-osmotically replaced NaCl) to block voltage-gated Na^+ channels. All signals
225 were acquired at 20 kHz and low-pass filtered at 10 kHz via a MultiClamp 700B amplifier. Data
226 were collected from the neurons with an input resistance >100 MΩ. If the series resistance for a
227 given recording was >30 MΩ or changed by more than 20%, the data were rejected for analysis.
228 The current and voltage signals were recorded and digitized with a MultiClamp 700B amplifier
229 and Digitdata 1440 controlled by Clampex 10 data acquisition software (Molecular Devices, San
230 Jose, CA, USA). For 5-6 weeks old LC excitability and CRF response recordings, baseline
231 excitability was collected 5 minutes after whole-cell and after evoked current injections (from -30
232 pA, increasing by 10 pA up to 100 pA with 10 seconds between each sweep) to ensure stable
233 recordings and complete dialysis of the cytosolic space with intracellular solution. CRF responses
234 were collected within 10 minutes following 500 nM CRF (human, rat, AnaSpec, Fremont, CA,
235 USA) applied in the ACSF bath application. For recordings from 7-8-week old mice, spontaneous
236 firing rates were collected first during a 3-5-minute free run, with sweeps excluded if they were
237 20% different from the average firing rate. Evoked firing responses to current injection steps were
238 next performed using the same protocol as previously described. IN current-clamp mode, the
239 neuronal membrane potential was kept at -60 mV by injecting an additional holding current, then
240 the same current injection protocol was performed. The action potential threshold was determined

241 by taking the average potential at which the dV/dt reached 20mV/ms when neurons fired
242 spontaneously. To determine the resting membrane, an all-points histogram was generated for
243 the spontaneous firing recording and the peak of the histogram (0.5 mV bins) was identified as
244 the resting potential in highly active neurons. Neuronal membrane resistance was determined
245 based on the holding current required for 5 mV step in voltage-clamp mode.

246 *Quantification and statistical analysis*

247 All data were evaluated with two- or three-way ANOVAs or repeated measures ANOVAs
248 (RMANOVAs), results of which are reported in **Supplementary Table 1**. If Spearman's test for
249 heteroscedasticity and the Shapiro-Wilk test for normality were not significant ($p > 0.05$), paired
250 t-tests (drug effects), unpaired t-tests (stress effects), or Fisher's Exact tests were used for
251 pairwise comparisons as indicated. If either Spearman's or the Shapiro-Wilk test were significant
252 ($p < 0.05$), a Wilcoxon Signed Rank Test for paired data (dug effects) or Mann-Whitney U test for
253 unpaired data were used for pairwise comparisons. Alpha levels of $p < 0.05$ were considered
254 significant for all main effects and pairwise comparisons, and $p < 0.10$ was considered significant
255 only for interactions when the main effects of stress had $p < 0.05$ in ANOVAs (**Figure 1c** and **2f**).
256 All results are expressed as the mean ± SEM and individual data points represent individual
257 animals in behavioral assays or neurons in cellular assays. Analyses and graphing were
258 conducted in Clampfit 10.0 (Molecular Devices, San Jose, CA, USA), Easy Electrophysiology
259 (Easy Electrophysiology Ltd, London, UK), Prism (10.0.2, Graphpad, Boston, MA, USA), and Igor
260 Pro 8 (WaveMetrics, Lake Oswego, OR, USA)

261

262 **Results**

263 *ELVS induces hyperactivity in a non-novel environment and impaired short-term memory with*
264 *female-specific increased exploratory and anhedonia-like behavior.*

265 To determine how early life stress impacts affective, cognitive, and locomotive behaviors
266 of male and female mice, we exposed C57Bl/6J (B6J) mice to a two-phase stress paradigm during

267 early life (P6-16) and adolescence (P28-P42) as described. At 6-7 weeks of age, male and female
268 control (handled daily) and ELVS mice were evaluated on a behavioral battery, including open
269 field (OF), Y-maze, elevated zero maze (EZM), novel object recognition (NOR), sucrose
270 preference (SP), and rotarod. Female ELVS mice displayed an increase in OF distance moved
271 (**Figure 1a-c**) when compared to female controls that persisted across the 30 min trial and was
272 absent in male mice. In contrast, total locomotion in the familiar open field after the third exposure
273 (habituation phase of NOR) was significantly increased in ELVS-exposed mice, regardless of sex,
274 indicating the development of hyperactivity in a familiar environment due to ELVS exposure.
275 Female ELVS mice also entered the center of the open field arena more frequently than control
276 females (**Figure 1e**), consistent with total OF locomotion. Mice of both sexes spent similar
277 amounts of time in the center of the OF, regardless of ELVS exposure (**Figure 1f**), suggesting a
278 lack of increased anxiety-like behavior despite ELVS exposure. Consistent with OF center time
279 and absence of anxiety-like behavior, there were no significant differences between groups in the
280 cumulative duration of time spent in the open arms of the elevated zero maze (**Figure 1g, h**). In
281 the Y-maze (**Figure 1i-k**), ELVS-exposed mice of both sexes demonstrated increased arm entries
282 (**Figure 1j**) and decreased correct arm alternation sequences (**Figure 1k**), indicating modestly
283 impaired short-term memory relative to control mice. There were no significant sex- or stress-
284 related differences observed in 24 hr novel object recognition (NOR, **Supp. Figure 1a-d**) or
285 rotarod latency to fall times (**Supp. Figure 1e-g**), which tested long-term (24 hr) memory and
286 motor function/coordination, respectively.

287 Following innate behavioral testing at 6 weeks of age, 7-week-old mice were water
288 restricted for two weeks, then completed sucrose preference testing. Only female ELVS mice
289 displayed a significant reduction in sucrose preference (**Figure 1m**) relative to control mice, which
290 suggests ELVS induces an anhedonia-like state in female mice. Overall, in mice of both sexes at
291 1.5 – 2 months of age, ELVS exposure led to increased exploratory activity and impaired short-
292 term memory, both ADHD-relevant behavioral domains. In parallel, hyperactivity and anhedonia-

like behavior were observed specifically in female mice, indicating changes in affective behavior due to a previous exposure to dual-phase ELVS.

ELVS exposure results in male-specific increases in impulsivity and female-specific deficits in attention.

Mice continued to be water restricted for the five-choice serial reaction time task (5CSRTT) training and testing. There was no effect of stress on the time necessary for mice to reach the criterion threshold (>80% accuracy and <30% omitted trials; **Figure 1a**). Although there were group effects of stress and sex on the total time to complete all training and testing sessions (**Figure 1b**), there were no significant ELVS effects on these metrics for either sex. As a measure of impulsivity, we evaluated the number of premature nosepoke responses for the first training trial when the stimulus duration and intertrial interval were shortened (**Figure 1c**), where we found that premature responses increased in males exposed to ELVS in contrast to being decreased in ELVS-exposed females. Once the mice had been trained to criterion on standard parameters, mice were evaluated in 5CSRTT sessions with varied parameters across ten different test sessions. Accuracy and trial omissions were similar for all groups on most test sessions (**Supp. Figure 2**), including those with short stimulus duration (**Figure 1d**, **g**). However, when the intertrial interval was reduced, ELVS-exposed mice of both sexes performed with similar accuracy (**Figure 2e**), but omitted significantly more trials (**Figure 2h**). 5CSRTT response accuracy was also reduced in ELVS female mice when session parameters were challenging with longer intertrial intervals in the presence of an audio distractor and the target brightness was varied (**Figure 2f**), with no changes in omissions (**Figure 2i**). These behavioral data demonstrate how ELVS exposure leads to male-specific increases in impulsivity while impairing specific attention parameters in ELVS females, suggesting sexually dimorphic effects of ELVS on specific neural circuits responsible for these behavioral changes.

318 *Corticotropin-releasing factor (CRF) directly excites noradrenergic neurons based on ELVS*
319 *exposure and via different signaling pathways in male and female mice.*

320 Based on previous studies showing the LC's involvement in affective and attentive
321 behaviors [35, 49, 50] and sex differences in second messenger pathways mediating CRF effects
322 in LC neuron [32], we further probed this sex difference during adolescence to determine the
323 degree to which CRF-evoked changes in LC excitability is dependent on sex and ELVS exposure.
324 To determine the accuracy of targeting putative noradrenergic LC neurons recorded in wildtype
325 B6J mice, we assess CRF (500 nM) effects on LC neuron activity using transgenic mice
326 expressing tdTomato driven by noradrenergic marker, dopamine β-hydroxylase (Dbh-tdTomato
327 mice) (**Figure 3a** & **b**). Baseline and CRF-induced changes in firing behavior of tdTomato+
328 noradrenergic LC neurons were similar to baseline and CRF-induced changes in B6J mice of both
329 sexes (**Figure 3c-g**). Because the generation of Dbh-tdTomato mice relies on a knock-in of Cre
330 in place of one copy of the *Dbh* gene, mechanistic studies were not performed in these mice due
331 to potential compensatory changes that may occur in the absence of one copy of *Dbh*. In B6J
332 mice, we controlled for whole cell configuration alterations in the internal cell conditions by
333 performing cell-attached recordings of responses to CRF bath applications, with CRF responses
334 similar to whole cell results (**Supp. Figure 3a**). There were also no significant changes in
335 spontaneous firing rate when cells were held in the whole cell condition (**Supp. Figure 3b**),
336 suggesting that this did not confound the observed firing changes upon CRF application.

337 To determine how ELVS exposure impacts CRF-induced LC neuron excitability changes,
338 we performed the same protocol of bath-applying CRF (500 nM) onto LC neurons of ELVS mice
339 at 6 weeks of age after completion of the ELVS protocol. While ELVS male LC neurons were still
340 responsive to CRF, there was a significant interaction between sex and stress on the effects of
341 CRF on spontaneous firing, with ELVS female LC neurons no longer responding by a change in
342 firing rate (**Figure 3e-g**). Sex differences in LC neuron CRF sensitivity may depend on sexually

343 dimorphic variations in CRF actions on LC neurons, which may shift after exposure to stress of
344 different types and timing in early life.

345 Although it has previously been reported that female LC CRFR1 receptor is predominantly
346 coupled to the G_s pathway [51–53], since CRFR1 can couple to G_s, G_q, and G_i pathways, we went
347 on to determine the role of G_q and G_s signaling in CRF-induced increases in LC neuron excitability
348 in both sexes. To determine G_q pathway dependence of CRF effects on excitability, a protein
349 lipase C (PLC) inhibitor 10 μM U73122 was added to the internal solution. In the presence of the
350 PLC inhibitor, bath application of 500 nM CRF no longer increased spontaneous firing of male
351 noradrenergic neurons (**Figure 3h** & **i**). In contrast, the inclusion of the PLC inhibitor had no effect
352 on CRF-induced changes in the spontaneous firing behavior of female noradrenergic LC neurons
353 (**Figure 3h & i**). 10 μM NF 449, a $G\alpha_s$ inhibitor [54], was next added to the internal pipette solution
354 to determine dependence of G_s-mediated signaling in CRF-induced excitability changes. CRF no
355 longer significantly increased female LC neurons' spontaneous firing in the presence of NF 449,
356 but CRF still significantly increased spontaneous firing in LC neurons from males (**Figure 3j** & **k**).
357 CRF did not have a robust effect on evoked firing in any groups or pharmacological treatments,
358 except in naïve males with NF449 added to the internal (**Supp. Figure 4**), which is consistent with
359 changes in spontaneous firing in response to CRF. Together, these data suggest that CRF
360 preferentially signals through G_q signaling pathways in males and G_s signaling pathways in
361 females, which may explain how stress signaling may lead to sexually dimorphic long-term
362 changes.

363 *ELVS Female LC Neurons are less excitable after stress and show increased action potential*
364 *delay attributed to A-type potassium channels.*

365 Given the sexual dimorphism of the behavioral phenotype produced by ELVS, sex
366 differences in LC neurons' CRF sensitivity, female-specific ELVS effects on LC neuronal CRF
367 sensitivity, and the lack of excitatory or inhibitory synaptic activity differences after stress (**Supp.**
368 **Figure 5**), we next assessed current clamp recordings from putative LC noradrenergic neurons

369 in *ex vivo* acute brain slices to determine whether ELVS produced persistent sex-specific changes
370 in excitability. At 6 weeks of age, immediately following stress, there were no clear changes
371 observed in LC neuron excitability (**Supp. Figure 6**), although at 7-8 weeks of age we found
372 robust ELVS-induced female-specific changes in LC neuron activity (**Figure 4**). Noradrenergic LC
373 neurons from female ELVS mice, but not males, displayed reduced spontaneous firing rates when
374 compared to controls (**Figure 4a** & **b)** with no changes in resting membrane potential (V_m; **Figure**
375 **4c**). Surprisingly, the membrane resistance was higher and the action potential (AP) threshold
376 more depolarized in ELVS female LC neurons (**Figure 4d** & **e**). Both male and female ELVS LC
377 neurons displayed modest, but significantly increased AP half-width (**Figure 4g**). LC neurons from
378 ELVS females also elicited fewer action potentials in response to current injection compared to
379 controls, a change which was absent in males (**Figure 4h-l**).

380 Since the resting potential of LC neurons was quite variable, in the same population of
381 neurons we also recorded evoked action potential firing when constant current was injected to
382 maintain the membrane potential at -60 mV to identify specifically how excitability may change
383 when controlling for V_m. From an initial resting potential of -60 mV in all neurons, ELVS females
384 continued to show reduced evoked excitability (**Figure 4o-q**), while absent in males (**Figure 4o**)
385 this excitability change appeared to be due to an increase in the delay time to the first action
386 potential following current injection in females (**Figure 4s & t**), at least in part. Although the delay
387 time to the first action potential was variable in all groups, almost all LC neurons in female ELVS
388 mice displayed a notable delay (>40-50 ms) in response to 70 pA current injection, while LC
389 neurons from animals in all other groups displayed both no delay and long delays (**Figure 4t**).
390 This highlights a female-specific LC physiology change that could contribute to the observed
391 sexually dimorphic LC-involved behavioral differences, potentially due to changes in distal release
392 of NE throughout the brain.

393 To determine the mechanism involved in reducing excitability and increased action
394 potential delay time in ELVS female LC neurons, we first investigated the role of ATP-sensitive

395 K+ channels, which could account for changes in excitability, by removing both cyclic nucleotides
396 (ATP and GTP) from the internal solution to promote maximal K_{ATP} activity and reduce variations
397 in activity that could alter membrane resistance and V_m (**Supp. Figure 7**). Although removing ATP
398 altered some stress effects on certain action potential properties, such as the action potential
399 threshold, the medium after hyperpolarization (mAHP) amplitude, and the action potential
400 halfwidth, female ELVS LC neurons remained less excitable both at their resting potential (**Supp.**
401 **Figure 4i**, **k**, **l**) and at -60 mV (**Supp. Figure 4n**, **p**, **q**). Importantly, the sex-specific ELVS-induced
402 increase in action potential delay time also persisted (**Supp. Figure 7r-t**). It is worth noting the
403 ELVS males showed a significant reduction in spontaneous firing rate when compared to controls
404 when ATP and GTP were excluded, but did not show any significant differences in evoked firing
405 at rest or at -60 mV (**Supp. Figure 7**).

406 Since action potential delays and suppression of firing rate in response to depolarizing
407 current are due to the activation of transient A-type voltage-gated potassium (K_v) channel-
408 mediated currents (I_A) known to be present in LC neurons and modifiable [55–57], we
409 pharmacologically assessed the I_A-dependence of this delay with 4-aminopyridine (4-AP, 1 mM).
410 To determine if this difference in A-type potassium channels contributes to the increase in action
411 potential delay time in ELVS females, we recorded current-injection evoked action potentials from
412 a V_m of -60 mV before and after bath application of 4-AP (1 mM) to block these transiently
413 activated channels (**Figure 5a**). In nearly all neurons from each group, 4-AP significantly reduced
414 the action potential delay time (**Figure 5b-f**), except for male ELVS mice where the delay time
415 was already short. In the presence of 4-AP, the action potential delay times were comparable in
416 all groups (**Figure 5f**). These data indicate that the 4-AP-sensitive increased action potential delay
417 time in ELVS female LC neurons is due to some change in expression or modulation of the K_v
418 channel or accessory protein mediating I_A that occurs due to ELVS exposure.

419 *Restoration of extracellular NE levels by reboxetine ameliorated ELVS-induced changes in*
420 *behavior.*

421 Electrophysiological recordings of LC neurons indicate a reduced excitability and
422 increased delay to respond to current injection, both of which would lead to reduced distal NE
423 release. Therefore, to determine the impact of these physiological changes on behavior, we
424 assessed whether increasing norepinephrine levels at noradrenergic synapses using reboxetine,
425 a selective norepinephrine reuptake inhibitor, would restore behaviors found to be altered in
426 separate cohorts of control and ELVS mice (**Figure 6**). We found that 2mg/kg oral reboxetine
427 administration restored female-specific effects of ELVS on sucrose preference behavior (**Figure**
428 **6a** & **b**). Oral reboxetine also significantly reduced exploratory behavior in ELVS mice (**Figure 6c**
429 & **d**), but did not alter y-maze performance (**Figure 6e** & **f**). Overall, this indicates that
430 manipulating the LC-NE system in a manner that is targeted based on the sex- and stress-
431 dependent changes in physiology may be beneficial in restoring specific affective behavioral
432 changes.

433 **Discussion**

434 *Summary of Findings*

435 In our two-phase animal model developed to mimic ACE-relevant timing of and systematic
436 variation in exposure to threat and deprivation in early life in mice, we identified altered exploratory
437 locomotion in a familiar environment, short-term memory in early adulthood, and evidence of
438 reduced ability to maintain attention, regardless of sex (**Figures 1 & 2**). We also found male-
439 specific increases in impulsivity and evidence of female-specific reduced impulsivity, increased
440 exploratory behavior, and an anhedonia-like state (**Figures 1 & 2**). Notably, changes in basal
441 anxiety-like behaviors were absent due to ELVS exposure in the B6J mice used here, in contrast
442 to Balb/C mice used in our previous work [58], where a prominent increase in anxiety-like behavior
443 was observed in female mice. Motivated by the role of norepinephrine release from the LC in
444 shaping these behaviors, our evaluation of LC neurons in these mice using electrophysiological
445 recordings identified a reduction in LC neuron excitability that was due in part to a prolongation of
446 the onset action potential delay (**Figure 4**), which was mediated by a 4-AP-sensitive A-type Kv

447 channel (**Figure 5**). Unlike male Balb/C mice exposed to a similar ELVS protocol [58], basal
448 properties of LC neurons from B6J male mice exposed to ELVS were remarkably similar to those
449 from control mice. In addition to blunted CRF sensitivity specifically in female mice exposed to
450 ELVS, in LC neurons from naïve mice, CRF-induced excitability changes were due to involvement
451 of sex-specific signaling pathways (**Figure 3**), which may partly explain why exposure to stressful
452 stimuli during adolescence leads to sex-specific changes in basal LC neuron excitability. Finally,
453 pharmacologically compensating for this loss of LC neuron excitability/NE release by blocking NE
454 reuptake with reboxetine [59] restored a subset of ELVS-induced behavioral changes (**Figure 6**),
455 a drug that has been used clinically to treat depression, panic disorder, and ADHD [60–62] with
456 variable success. Together, these data highlight the dynamics and importance of understanding
457 the complex interplay between sex, age (critical periods), genotypic variation, stress exposure,
458 and neuromodulator circuit changes.

459 *The Impact of Stress and Sex on LC Function Related to Affect and Cognition*

460 The LC-NE system is also well-documented to be stress-sensitive, as it is activated by an
461 array of environmental stressors, including social and predator stress [19, 21, 63–69]. Largely
462 limited to stress exposure in males, acute stress-induced changes in LC_{NE} activity is proposed to
463 occur primarily through the activation of $CRFR_1$ by CRF released from several brain areas,
464 including the central amygdala and paraventricular nucleus of the hypothalamus [19, 64, 70–73].
465 At least in male rats, stress and stress-related CRF release shift LC activity towards a high tonic
466 firing mode (3-8 Hz) while simultaneously decreasing phasic firing events [72, 74, 75]. These
467 stress-induced increases in CRF and modulation of LC-NE neuron activity are paralleled by CRF-
468 induced changes in multiple processes and behaviors known to be heavily shaped by LC-NE
469 neuron activity, including attention [76], cognitive flexibility [19], anxiety [10, 15], and memory [77].
470 The data presented here shed light on how the LC-NE system changes with multiple early life
471 stress exposures, and likely related increase in CRF release, depending on sex.

472 The nature of the LC physiology changes of female mice due to ELVS exposure has the
473 potential to affect both tonic and phasic firing, each of which is proposed to be related to specific
474 behavioral events [16, 17, 28, 78]. First, the reduced LC spontaneous and persistent evoked firing
475 rate observed only in ELVS-exposed females will affect tonic firing. Second, by reducing the
476 likelihood of generating an action potential in response to short depolarizing events (i.e. the
477 beginning of current injection steps), the prolongation of the action potential delay time will act as
478 a filter of fast synaptic inputs to reduce the likelihood of phasic firing and subsequent distal NE
479 release. By disrupting both types of LC neuron firing modes, these changes observed in females
480 could result in disrupted NE signaling in multiple brain regions involved in attention, arousal,
481 memory, and/or locomotion (i.e. prefrontal cortex, hippocampus, ventral tegmental area, and
482 lateral cerebellar nucleus).

483 Although LC-NE neurons were previously thought to be a homogenous population, recent
484 data suggest that they are much more heterogeneous in their molecular [79] or functional
485 properties that relate to specific LC-NE projection targets [80, 81]. Given the range of delay times,
486 resting potentials, and spontaneous firing rates observed in this population of LC neurons, it
487 appears that ELVS exposure leads to a shift in the distribution of these key properties across the
488 population, likely due to sex-specific variation in CRF-activated signaling. However, it is not clear
489 how a change in these functional properties may relate to changes in specific molecularly-,
490 anatomically- (target brain area), or functionally-defined LC neuron sub-populations. Whether
491 acute or persistent changes in the physiological properties of LC-NE neurons and/or their synaptic
492 properties, like those observed here, may impact NE release throughout the central nervous
493 system differentially based on specific circuits or related behavior is unclear. Since there is a
494 smaller distribution of firing rates yet lager distribution of action potential delay times across LC
495 neurons in ELVS females when compared to controls, this property-dependent shift in the
496 functional diversity of LC neurons could impact how firing modes required for optimal projecting
497 brain region states. For instance, distinct LC ensembles projecting to the cortex may modulate

498 particular cortical states with members of each ensemble having definitive firing rates [82]. Further
499 effort to determine exactly how these changes in LC-NE system excitability alter widespread
500 noradrenergic signaling *in vivo* during specific behaviors would provide support for the importance
501 of this physiological change and suggest the LC-NE system to be a female-specific target of
502 interest for stress-related disorders, particularly with onset after adolescence.

503 The specific sexually dimorphic molecular mechanisms underpinning LC physiology
504 changes after exposure to the ELVS are still unclear. However, our results in naïve mice (**Figure**
505 **3**) establish that there are basal sex differences in how CRF exposure affects the firing of LC
506 neurons, at least in the signaling pathways involved in CRF-induced increases in firing rate,
507 indicating preferential G_q signaling in males and G_s in females. These data are in line with other
508 reports of female CRFR1 in the LC being predominantly G_s-coupled and males having increased
509 β-arrestin-related internalization of CRFR1 after acute stress [32]. Bridging the gap in future work
510 to understand how two-phase early life stress and acute stress affect CRF-dependent changes in
511 LC physiology and related signaling based on sex will be important to understand fundamental
512 sex-specific processes that shape responses to stress on both timescales. Based on these data,
513 we predict that the predominant G_s-dependent CRF actions in females, leading to PKA activation,
514 will cause unique subsequent and persistent changes in LC physiology (excitability, delay) in
515 females that will be absent in males. In parallel, the G_q coupling predominance could be protective
516 in males due to its transient Ca^{2+}-dependent action versus a prolonged upregulation of a signaling
517 cascade. Given recent reports of persistent LC physiology changes occurring only when stress
518 exposure happens at adolescence and not adulthood [83], determining the degree to which this
519 applies to our dual-phase ELVS paradigm and the duration of any lasting behavioral and
520 physiological changes will also be important to understand dynamics that shape the broader
521 impacts of stress. Finally, at a molecular level, it is unclear how exactly I_A is modulated or affected
522 by stress, but clarifying the channels and auxiliary subunit changes over longer time scales may

523 reveal novel mechanisms of broader and LC-specific responses to critically-timed stress to shape
524 novel prevention and treatment strategies to improve specific behavioral outcomes.

525 *Clinical Impact of Findings*

526 The treatment of stress- or specifically ACE-related disorders should consider sex and the
527 timing of stress exposure as biological variables influencing patient outcomes. These behavioral
528 results suggest females may be more sensitive to depression-like behaviors and ADHD-relevant
529 deficits as a result of early life stress during comparable time periods used in this study. Based
530 on these data, individuals exposed to ACEs as adolescents may be particularly sensitive to
531 developing negative neuropsychiatric outcomes later in life, based on sex differences in LC
532 neuron physiology and central stress (CRF) sensitivity at this time. Regardless, the specific role
533 of sex hormones in development and neurophysiological changes in response to stress is unclear.
534 Estrogen receptor α (ERα) and β (ERβ) are differentially expressed in the amygdala, prefrontal
535 cortex, and hippocampus responsible for stress, anxiety, and cognitive behaviors, respectively
536 [84]. ERβ has been associated with non-reproductive behaviors, with its activation improving
537 memory and reducing anxious behaviors in females [85, 86]. In contrast, testosterone signaling
538 has been suggested to be a factor supporting resilience to stress-induced changes, which is in
539 line with the behavioral data presented here [87, 88].

540 This study may implicate the adrenergic system, particularly the LC in the brain, as a
541 region to explore biomarkers of dysfunction in female patients with a history of stress in early life.
542 According to the DSM-V, cognitive issues are a core symptom of depression that include aspects
543 of memory and attention being disrupted [89, 90]. These symptoms are in line with the female-
544 specific behavioral impacts of our dual-phase stress model, pointing to increasing noradrenergic
545 tone as a therapeutic avenue for treatment. There are many drugs that target this brain area,
546 particularly second-line therapies for attention deficit hyperactivity disorder (ADHD), such as
547 reboxetine [61] used in this study, which may prove to be effective in managing cognitive
548 impairments in this patient group with depression and/or PTSD. These data provide a foundation

549 for further research into neuro-stress regulation differences in males and females, relevant to
550 many stress-related disorders, from PTSD to substance abuse disorder, that have sex differences
551 in their prevalence ratios [46]. Perhaps a more robust individualized understanding of how
552 patients' genetic and environmental risk factors interact with the type of timing of major stressful
553 life events may increase the likelihood of therapeutic success when these variables are used to
554 optimize drug choice.
555

556 **Acknowledgements**

557 This work was supported by institutional start-up funds and a Research Seed Grant from SIU-

558 School of Medicine provided to BDR.

559 **Conflict of Interest**

560 Neither author has any conflicts of interest to declare.

561 **References**

562 1. Pitts BL, Eisenberg ML, Bailey HR, Zacks JM. PTSD is associated with impaired event
563 processing and memory for everyday events. Cognitive Research: Principles and
564 Implications. 2022;7:35.

565 2. Vesga-López O, Blanco C, Keyes K, Olfson M, Grant BF, Hasin DS. Psychiatric Disorders in
566 Pregnant and Postpartum Women in the United States. Archives of General Psychiatry.
567 2008;65:805.

568 3. Hickey M, Bryant C, Judd F. Evaluation and management of depressive and anxiety
569 symptoms in midlife. Climacteric. 2012;15:3–9.

570 4. Aston-Jones G, Rajkowski J, Kubiak P, Alexinsky T. Locus coeruleus neurons in monkey are
571 selectively activated by attended cues in a vigilance task. The Journal of Neuroscience :
572 The Official Journal of the Society for Neuroscience. 1994;14:4467–4480.

573 5. Kuo C-C, Hsieh J-C, Tsai H-C, Kuo Y-S, Yau H-J, Chen C-C, et al. Inhibitory interneurons
574 regulate phasic activity of noradrenergic neurons in the mouse locus coeruleus and
575 functional implications. The Journal of Physiology. 2020;598:4003–4029.

576 6. Borodovitsyna O, Duffy BC, Pickering AE, Chandler DJ. Anatomically and functionally
577 distinct locus coeruleus efferents mediate opposing effects on anxiety-like behavior.
578 Neurobiology of Stress. 2020;13.

579 7. Poe GR, Foote S, Eschenko O, Johansen JP, Bouret S, Aston-Jones G, et al. Locus coeruleus:
580 a new look at the blue spot. Nat Rev Neurosci. 2020;21:644–659.

581 8. Chandler DJ, Jensen P, McCall JG, Pickering AE, Schwarz LA, Totah NK. Redefining
582 Noradrenergic Neuromodulation of Behavior: Impacts of a Modular Locus Coeruleus
583 Architecture. J Neurosci. 2019;39:8239–8249.
584 9. Breton-Provencher V, Drummond GT, Sur M. Locus Coeruleus Norepinephrine in Learned
585 Behavior: Anatomical Modularity and Spatiotemporal Integration in Targets. Frontiers in
586 Neural Circuits. 2021;15.
587 10. McCall JG, Siuda ER, Bhatti DL, Lawson LA, McElligott ZA, Stuber GD, et al. Locus coeruleus
588 to basolateral amygdala noradrenergic projections promote anxiety-like behavior. eLife.
589 2017;6.
590 11. Ishida Y, Shirokawa T, Miyaishi O, Komatsu Y, Isobe K. Age-dependent changes in
591 projections from locus coeruleus to hippocampus dentate gyrus and frontal cortex. The
592 European Journal of Neuroscience. 2000;12:1263–1270.
593 12. Lim EP, Tan CH, Jay TM, Dawe GS. Locus coeruleus stimulation and noradrenergic
594 modulation of hippocampo-prefrontal cortex long-term potentiation. The International
595 Journal of Neuropsychopharmacology. 2010;13:1219–1231.
596 13. Mair RD, Zhang Y, Bailey KR, Toupin MM, Mair RG. Effects of clonidine in the locus
597 coeruleus on prefrontal- and hippocampal-dependent measures of attention and memory
598 in the rat. Psychopharmacology. 2005;181:280–288.
599 14. Dornellas APS, Burnham NW, Luhn KL, Petruzzi MV, Thiele TE, Navarro M. Activation of
600 locus coeruleus to rostromedial tegmental nucleus (RMTg) noradrenergic pathway blunts
601 binge-like ethanol drinking and induces aversive responses in mice. Neuropharmacology.
602 2021;199.

603 15. Borodovitsyna O, Duffy BC, Pickering AE, Chandler DJ. Anatomically and functionally
604 distinct locus coeruleus efferents mediate opposing effects on anxiety-like behavior.
605 Neurobiology of Stress. 2020;13.
606 16. Rajkowski J, Kubiak P, Aston-Jones G. Locus coeruleus activity in monkey: phasic and tonic
607 changes are associated with altered vigilance. Brain Research Bulletin. 1994;35:607–616.
608 17. Howells FM, Stein DJ, Russell VA. Synergistic tonic and phasic activity of the locus
609 coeruleus norepinephrine (LC-NE) arousal system is required for optimal attentional
610 performance. Metabolic Brain Disease. 2012;27:267–274.
611 18. McBurney-Lin J, Vargova G, Garad M, Zagha E, Yang H. The locus coeruleus mediates
612 behavioral flexibility. Cell Rep. 2022;41:111534.
613 19. Snyder K, Wang W-W, Han R, McFadden K, Valentino RJ. Corticotropin-releasing factor in
614 the norepinephrine nucleus, locus coeruleus, facilitates behavioral flexibility.
615 Neuropsychopharmacology. 2012;37:520–530.
616 20. Su Z, Cohen JY. Two types of locus coeruleus norepinephrine neurons drive reinforcement
617 learning. 2022.
618 21. McCall JG, Al-Hasani R, Siuda ER, Hong DY, Norris AJ, Ford CP, et al. CRH Engagement of
619 the Locus Coeruleus Noradrenergic System Mediates Stress-Induced Anxiety. Neuron.
620 2015;87:605–620.
621 22. Pasquier DA, Reinoso-Suarez F. The topographic organization of hypothalamic and brain
622 stem projections to the hippocampus. Brain Research Bulletin. 1978;3:373–389.
623 23. Fitzpatrick CM, Runegaard AH, Christiansen SH, Hansen NW, Jørgensen SH, McGirr JC, et
624 al. Differential effects of chemogenetic inhibition of dopamine and norepinephrine

625 neurons in the mouse 5-choice serial reaction time task. Progress in Neuro-
626 Psychopharmacology & Biological Psychiatry. 2019;90:264–276.
627 24. Uematsu A, Tan BZ, Ycu EA, Cuevas JS, Koivumaa J, Junyent F, et al. Modular organization
628 of the brainstem noradrenaline system coordinates opposing learning states. Nature
629 Neuroscience. 2017;20:1602–1611.
630 25. Campese VD, Soroeta JM, Vazey EM, Aston-Jones G, LeDoux JE, Sears RM. Noradrenergic
631 Regulation of Central Amygdala in Aversive Pavlovian-to-Instrumental Transfer. eNeuro.
632 2017;4.
633 26. Carlson ES, Hunker AC, Sandberg SG, Locke TM, Geller JM, Schindler AG, et al.
634 Catecholaminergic Innervation of the Lateral Nucleus of the Cerebellum Modulates
635 Cognitive Behaviors. The Journal of Neuroscience : The Official Journal of the Society for
636 Neuroscience. 2021;41:3512–3530.
637 27. Feng J, Dong H, Lischinsky JE, Zhou J, Deng F, Zhuang C, et al. Monitoring norepinephrine
638 release in vivo using next-generation GRABNE sensors. Neuron. 2024;112:1930-1942.e6.
639 28. Vazey EM, Moorman DE, Aston-Jones G. Phasic locus coeruleus activity regulates cortical
640 encoding of salience information. Proc Natl Acad Sci U S A. 2018;115:E9439–E9448.
641 29. Devilbiss DM, Page ME, Waterhouse BD. Locus Ceruleus Regulates Sensory Encoding by
642 Neurons and Networks in Waking Animals. J Neurosci. 2006;26:9860–9872.
643 30. Devilbiss DM, Waterhouse BD. The Effects of Tonic Locus Ceruleus Output on Sensory-
644 Evoked Responses of Ventral Posterior Medial Thalamic and Barrel Field Cortical Neurons
645 in the Awake Rat. J Neurosci. 2004;24:10773–10785.

646 31. Butler PD, Weiss JM, Stout JC, Nemeroff CB. Corticotropin-releasing factor produces fear-
647 enhancing and behavioral activating effects following infusion into the locus coeruleus. J
648 Neurosci. 1990;10:176–183.
649 32. Bangasser DA, Curtis A, Reyes BAS, Bethea TT, Parastatidis I, Ischiropoulos H, et al. Sex
650 differences in corticotropin-releasing factor receptor signaling and trafficking: potential
651 role in female vulnerability to stress-related psychopathology. Molecular Psychiatry.
652 2010;15:877, 896–904.
653 33. Valentino RJ, Foote SL, Aston-Jones G. Corticotropin-releasing factor activates
654 noradrenergic neurons of the locus coeruleus. Brain Research. 1983;270:363–367.
655 34. Wang Q, Liu Y, Zhang J, Wang W. Corticotropin-Releasing Factor Receptors in the Locus
656 Coeruleus Modulate the Enhancement of Active Coping Behaviors Induced by Chronic
657 Predator Odor Inoculation in Mice. Frontiers in Psychology. 2020;10.
658 35. Seo D, Zhang ET, Piantadosi SC, Marcus DJ, Motard LE, Kan BK, et al. A locus coeruleus to
659 dentate gyrus noradrenergic circuit modulates aversive contextual processing. Neuron.
660 2021;109:2116-2130.e6.
661 36. Breton-Provencher V, Drummond GT, Sur M. Locus Coeruleus Norepinephrine in Learned
662 Behavior: Anatomical Modularity and Spatiotemporal Integration in Targets. Frontiers in
663 Neural Circuits. 2021;15.
664 37. Lim EP, Tan CH, Jay TM, Dawe GS. Locus coeruleus stimulation and noradrenergic
665 modulation of hippocampo-prefrontal cortex long-term potentiation. The International
666 Journal of Neuropsychopharmacology. 2010;13:1219–1231.

667 38. McCall JG, Siuda ER, Bhatti DL, Lawson LA, McElligott ZA, Stuber GD, et al. Locus coeruleus
668 to basolateral amygdala noradrenergic projections promote anxiety-like behavior. eLife.
669 2017;6.
670 39. Fortress AM, Hamlett ED, Vazey EM, Aston-Jones G, Cass WA, Boger HA, et al. Designer
671 receptors enhance memory in a mouse model of Down syndrome. The Journal of
672 Neuroscience : The Official Journal of the Society for Neuroscience. 2015;35:1343–1353.
673 40. Mariscal P, Bravo L, Llorca-Torralba M, Razquin J, Miguelez C, Suárez-Pereira I, et al. Sexual
674 differences in locus coeruleus neurons and related behavior in C57BL/6J mice. Biol Sex
675 Differ. 2023;14.
676 41. Lee J, Wang Z, Messi ML, Milligan C, Furdui CM, Delbono O. Sex differences in single
677 neuron function and proteomics profiles examined by patch-clamp and mass spectrometry
678 in the locus coeruleus of the adult mouse. Acta Physiologica. 2024. 8 March 2024.
679 https://doi.org/10.1111/apha.14123.
680 42. Bangasser DA, Zhang X, Garachh V, Hanhauser E, Valentino RJ. Sexual dimorphism in locus
681 coeruleus dendritic morphology: a structural basis for sex differences in emotional
682 arousal. Physiology & Behavior. 2011;103:342–351.
683 43. Bangasser DA, Wiersielis KR, Khantsis S. Sex differences in the locus coeruleus-
684 norepinephrine system and its regulation by stress. Brain Research. 2016;1641:177–188.
685 44. Mulvey B, Bhatti DL, Gyawali S, Lake AM, Kriaucionis S, Ford CP, et al. Molecular and
686 Functional Sex Differences of Noradrenergic Neurons in the Mouse Locus Coeruleus. Cell
687 Reports. 2018;23:2225–2235.

688 45. Bangasser DA, Valentino RJ. Sex differences in stress-related psychiatric disorders:
689 neurobiological perspectives. Frontiers in Neuroendocrinology. 2014;35:303–319.
690 46. Swaab DF, Bao A-M. Sex differences in stress-related disorders: Major depressive disorder,
691 bipolar disorder, and posttraumatic stress disorder. Handbook of Clinical Neurology.
692 2020;175:335–358.
693 47. Tillage RP, Sciolino NR, Plummer NW, Lustberg D, Liles LC, Hsiang M, et al. Elimination of
694 galanin synthesis in noradrenergic neurons reduces galanin in select brain areas and
695 promotes active coping behaviors. Brain Struct Funct. 2020;225:785–803.
696 48. Madisen L, Mao T, Koch H, Zhuo J, Berenyi A, Fujisawa S, et al. A toolbox of Cre-dependent
697 optogenetic transgenic mice for light-induced activation and silencing. Nature
698 Neuroscience. 2012;15:793–802.
699 49. Aston-Jones G, Rajkowski J, Cohen J. Role of locus coeruleus in attention and behavioral
700 flexibility. Biological Psychiatry. 1999;46:1309–1320.
701 50. Hallock HL, Adiraju SS, Miranda-Barrientos J, McInerney JM, Oh S, DeBrosse AC, et al.
702 Electrophysiological correlates of attention in the locus coeruleus-prelimbic cortex circuit
703 during the rodent continuous performance test. Neuropsychopharmacology : Official
704 Publication of the American College of Neuropsychopharmacology. 2024;49:521–531.
705 51. Bangasser DA, Curtis A, Reyes BAS, Bethea TT, Parastatidis I, Ischiropoulos H, et al. Sex
706 differences in corticotropin-releasing factor receptor signaling and trafficking: potential
707 role in female vulnerability to stress-related psychopathology. Molecular Psychiatry.
708 2010;15:877, 896–904.

709 52. Bangasser DA, Wiersielis KR. Sex differences in stress responses: a critical role for
710 corticotropin-releasing factor. Hormones. 2018;17:5–13.
711 53. Bangasser DA, Valentino RJ. Sex differences in stress-related psychiatric disorders:
712 neurobiological perspectives. Frontiers in Neuroendocrinology. 2014;35:303–319.
713 54. Hohenegger M, Waldhoer M, Beindl W, Böing B, Kreimeyer A, Nickel P, et al. Gsalpha-
714 selective G protein antagonists. Proc Natl Acad Sci U S A. 1998;95:346–351.
715 55. Itri JN, Vosko AM, Schroeder A, Dragich JM, Michel S, Colwell CS. Circadian Regulation of
716 A-Type Potassium Currents in the Suprachiasmatic Nucleus. Journal of Neurophysiology.
717 2010;103:632–640.
718 56. Burdakov D, Ashcroft FM. Cholecystokinin Tunes Firing of an Electrically Distinct Subset of
719 Arcuate Nucleus Neurons by Activating A-Type Potassium Channels. J Neurosci.
720 2002;22:6380–6387.
721 57. Wu R-N, Hung W-C, Chen C-T, Tsai L-P, Lai W-S, Min M-Y, et al. Firing activity of locus
722 coeruleus noradrenergic neurons decreases in necdin-deficient mice, an animal model of
723 Prader–Willi syndrome. J Neurodevelop Disord. 2020;12.
724 58. Brannan S, Garbe L, Richardson BD. Early life stress induced sex-specific changes in
725 behavior is paralleled by altered locus coeruleus physiology in BALB/cJ mice. Neurobiology
726 of Stress. 2024;33.
727 59. Page ME. The promises and pitfalls of reboxetine. CNS Drug Rev. 2003;9:327–342.
728 60. Riahi F, Tashakori A, Izadi-Mazidi S, Salehi-Veysi M. Effectiveness of reboxetine in
729 treatment of outpatient children and adolescents with attention deficit-hyperactivity
730 disorder with comorbid anxiety disorders. Iran J Psychiatry. 2013;8:195–200.

731 61. Cohen-Yavin I, Yoran-Hegesh R, Strous RD, Kotler M, Weizman A, Spivak B. Efficacy of
732 Reboxetine in the Treatment of Attention-Deficit/Hyperactivity Disorder in Boys With
733 Intolerance to Methylphenidate. Clinical Neuropharmacology. 2009;32:179–182.
734 62. Block SG, Nemeroff CB. Emerging antidepressants to treat major depressive disorder.
735 Asian J Psychiatr. 2014;12:7–16.
736 63. Curtis a L, Bello NT, Valentino RJ. Evidence for functional release of endogenous opioids in
737 the locus ceruleus during stress termination. The Journal of Neuroscience : The Official
738 Journal of the Society for Neuroscience. 2001;21:RC152.
739 64. Curtis AL, Leiser SC, Snyder K, Valentino RJ. Predator stress engages corticotropin-releasing
740 factor and opioid systems to alter the operating mode of locus coeruleus norepinephrine
741 neurons. Neuropharmacology. 2012;62:1737–1745.
742 65. Bingham B, McFadden K, Zhang X, Bhatnagar S, Beck S, Valentino R. Early adolescence as a
743 critical window during which social stress distinctly alters behavior and brain
744 norepinephrine activity. Neuropsychopharmacology. 2011;36:896–909.
745 66. Borodovitsyna O, Flamini MD, Chandler DJ. Acute Stress Persistently Alters Locus
746 Coeruleus Function and Anxiety-like Behavior in Adolescent Rats. Neuroscience.
747 2018;373:7–19.
748 67. Cassens G, Roffman M, Kuruc A, Orsulak PJ, Schildkraut JJ. Alterations in brain
749 norepinephrine metabolism induced by environmental stimuli previously paired with
750 inescapable shock. Science. 1980;209:1138–1140.
751 68. Francis DD, Caldji C, Champagne F, Plotsky PM, Meaney MJ. The role of corticotropin-
752 releasing factor–norepinephrine systems in mediating the effects of early experience on

753 the development of behavioral and endocrine responses to stress. Biological Psychiatry.
754 1999;46:1153–1166.
755 69. George SA, Knox D, Curtis AL, Aldridge JW, Valentino RJ, Liberzon I. Altered locus
756 coeruleus–norepinephrine function following single prolonged stress. Eur J of
757 Neuroscience. 2013;37:901–909.
758 70. Valentino RJ, Van Bockstaele E. Convergent regulation of locus coeruleus activity as an
759 adaptive response to stress. Eur J Pharmacol. 2008;583:194–203.
760 71. Borodovitsyna O, Flamini MD, Chandler DJ. Acute Stress Persistently Alters Locus
761 Coeruleus Function and Anxiety-like Behavior in Adolescent Rats. Neuroscience.
762 2018;373:7–19.
763 72. Reyes BAS, Glaser JD, Bockstaele EJV. Ultrastructural evidence for co-localization of
764 corticotropin-releasing factor receptor and mu-opioid receptor in the rat nucleus locus
765 coeruleus. Neuroscience Letters. 2007;413:216–221.
766 73. Reyes B a. S, Carvalho AF, Vakharia K, Van Bockstaele EJ. Amygdalar peptidergic circuits
767 regulating noradrenergic locus coeruleus neurons: linking limbic and arousal centers. Exp
768 Neurol. 2011;230:96–105.
769 74. Reyes B a. S, Carvalho AF, Vakharia K, Van Bockstaele EJ. Amygdalar peptidergic circuits
770 regulating noradrenergic locus coeruleus neurons: linking limbic and arousal centers. Exp
771 Neurol. 2011;230:96–105.
772 75. Reyes BAS, Zitnik G, Foster C, Van Bockstaele EJ, Valentino RJ. Social Stress Engages
773 Neurochemically-Distinct Afferents to the Rat Locus Coeruleus Depending on Coping
774 Strategy,,. eNeuro. 2015;2.

775 76. Cole RD, Kawasumi Y, Parikh V, Bangasser DA. Corticotropin releasing factor impairs
776 sustained attention in male and female rats. Behavioural Brain Research. 2016;296:30–34.
777 77. Paretkar T, Dimitrov E. The Central Amygdala Corticotropin-releasing hormone (CRH)
778 Neurons Modulation of Anxiety-like Behavior and Hippocampus-dependent Memory in
779 Mice. Neuroscience. 2018;390:187–197.
780 78. Grimm C, Duss SN, Privitera M, Munn BR, Karalis N, Frässle S, et al. Tonic and burst-like
781 locus coeruleus stimulation distinctly shift network activity across the cortical hierarchy.
782 Nat Neurosci. 2024;27:2167–2177.
783 79. Hughes AC, Pittman BG, Xu B, Gammons JW, Webb CM, Nolen HG, et al. A single-vector
784 intersectional AAV strategy for interrogating cellular diversity and brain function. Nature
785 Neuroscience. 2024;27:1400–1410.
786 80. Waterhouse BD, Predale HK, Plummer NW, Jensen P, Chandler DJ. Probing the structure
787 and function of locus coeruleus projections to CNS motor centers. Front Neural Circuits.
788 2022;16:895481.
789 81. Chandler DJ, Gao W-J, Waterhouse BD. Heterogeneous organization of the locus coeruleus
790 projections to prefrontal and motor cortices. Proc Natl Acad Sci U S A. 2014;111:6816–
791 6821.
792 82. Noei S, Zouridis IS, Logothetis NK, Panzeri S, Totah NK. Distinct ensembles in the
793 noradrenergic locus coeruleus are associated with diverse cortical states. Proceedings of
794 the National Academy of Sciences. 2022;119.

795 83. Borodovitsyna O, Tkaczynski JA, Corbett CM, Loweth JA, Chandler DJ. Age- and Sex-
796 Dependent Changes in Locus Coeruleus Physiology and Anxiety-Like Behavior Following
797 Acute Stressor Exposure. Frontiers in Behavioral Neuroscience. 2022;16:808590.
798 84. Cover KK, Maeng LY, Lebrón-Milad K, Milad MR. Mechanisms of estradiol in fear circuitry:
799 implications for sex differences in psychopathology. Translational Psychiatry. 2014;4:e422.
800 85. Oyola MG, Portillo W, Reyna A, Foradori CD, Kudwa A, Hinds L, et al. Anxiolytic effects and
801 neuroanatomical targets of estrogen receptor-β (ERβ) activation by a selective ERβ agonist
802 in female mice. Endocrinology. 2012;153:837–846.
803 86. Jacome LF, Gautreaux C, Inagaki T, Mohan G, Alves S, Lubbers LS, et al. Estradiol and ERβ
804 agonists enhance recognition memory, and DPN, an ERβ agonist, alters brain monoamines.
805 Neurobiology of Learning and Memory. 2010;94:488–498.
806 87. Pfau ML, Russo SJ. Peripheral and Central Mechanisms of Stress Resilience. Neurobiology
807 of Stress. 2015;1:66–79.
808 88. Russo SJ, Murrough JW, Han M-H, Charney DS, Nestler EJ. Neurobiology of resilience.
809 Nature Neuroscience. 2012;15:1475–1484.
810 89. Perini G, Cotta Ramusino M, Sinforiani E, Bernini S, Petrachi R, Costa A. Cognitive
811 impairment in depression: recent advances and novel treatments. Neuropsychiatr Dis
812 Treat. 2019;15:1249–1258.
813 90. Mattingly G, Anderson RH, Mattingly SG, Anderson EQ. The impact of cognitive challenges
814 in major depression: the role of the primary care physician. Postgrad Med. 2016;128:665–
815 671.
816
817

818 **Figure**

819 *Figure 1*

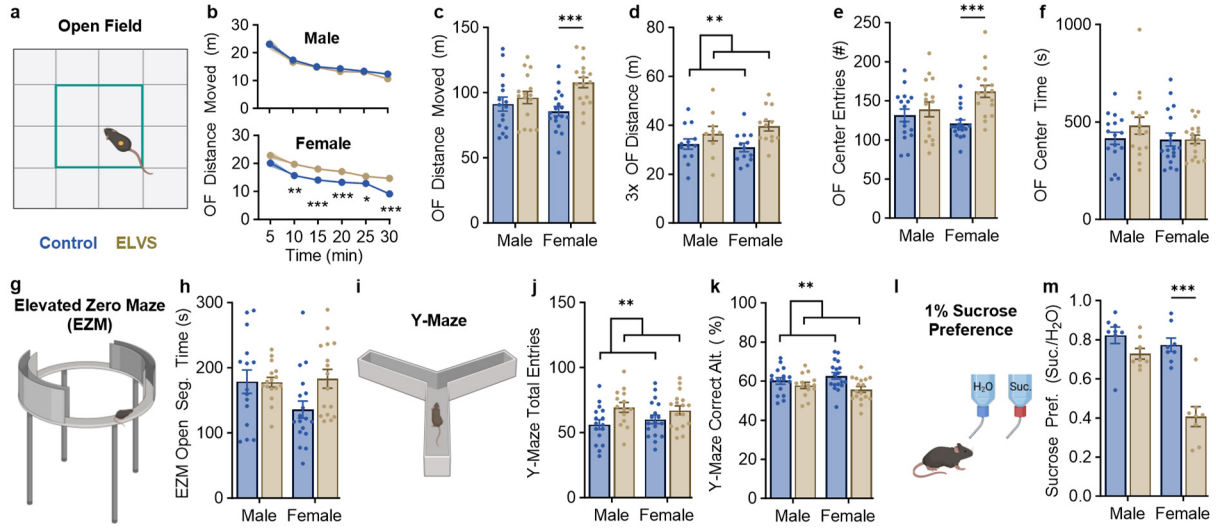

820

821 **Figure 1. ELVS causes sex-independent and female-specific changes in cognitive and**
822 **affective behavior.** (**a-c**) Total distance (meters, m) moved in the open field (OF) assay (**a**)
823 across the entire 30 min session (**b**; females: U = 48.0 – 92.0, p = 0.00030 – 0.045) and in total
824 (**c**; male: $t(30) = 0.70$, $p = 0.49$; female: $t(33) = 4.08$, $p = 0.0003$). (**d**) Total distance (m) moved in
825 OF apparatus during the third exposure (3x OF) for 10 minutes (combined: $t(47) = 3.13$, p =
826 0.0030). (**e**, **f**) The number of entries into (**e**; male: $t(30) = 0.63$, $p = 0.53$; female: $t(33) = 4.63$, p
827 < 0.0001) and total time spent (**f**) in the center of the OF arena. (**g**, **h**) Time (seconds) spent (**h**)
828 in the elevated zero maze (EZM, **g**) open arm. (**i-k**) Y-Maze (**i**) total number of arm entries (**j**;
829 combined: $t(63) = 2.83$, $p = 0.0063$) and correct arm alternation percentages (**k**; combined: $t(63)$
830 $= 2.94$, $p = 0.0046$). (**l**, **m**) Sucrose preference (**l**) index values as the ratio of 1% sucrose/H_2O
831 only (**m**: male: $t(14) = 1.89$, $p = 0.08$; female: $t(14) = 5.99$, $p < 0.0001$). All results are presented
832 as mean ± SEM for each group with circles representing data from individual mice. **a-k**: N = 10-
833 18 mice (6 weeks) per group. **m**: N = 8 mice (9 weeks) per group. *$p < 0.05$, **$p < 0.01$, ***$p <$
834 0.001 with two-tailed unpaired t-test or Mann-Whitney U test for pairwise comparisons.

835 *Figure 2*

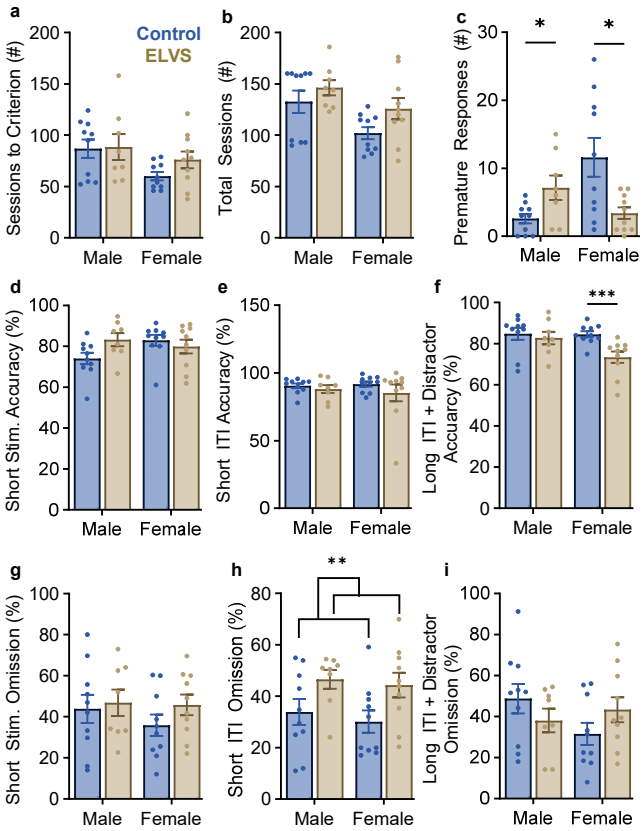

836

837 **Figure 2. ELVS leads to sexually dimorphic changes in impulsivity and female-specific**
838 **distractibility in 5-choice serial reaction time task (5CSRTT).** (**a**) Days needed to meet criteria
839 during 5CSRTT training. (**b**) Days required to complete training and all session variation tests
840 (male: $t(16) = 0.98$, $p = 0.34$; female: $t(18) = 2.02$, p 0.059). (**c**) Number of premature responses
841 during the first training transition session in 5CSRTT training with reduced stimulus duration and
842 intertrial interval (males: U = 15.0, $p = 0.024$; females: U = 22.0, p=0.033). Trial accuracy % (**d-f**)
843 and omission % (**g-i**) in test sessions with shortened stimulus duration in **d** and **g**, shortened
844 intertrial interval in **e** and **h** (combined: $t(36) = 2.97$, $p = 0.0053$), and lengthened intertrial interval
845 with a simultaneous sound distractor in **f** (male: U = 30.5, $p = 0.42$; female: U = 9.0, p=0.0010)
846 and **i**.

847

848 *Figure 3*

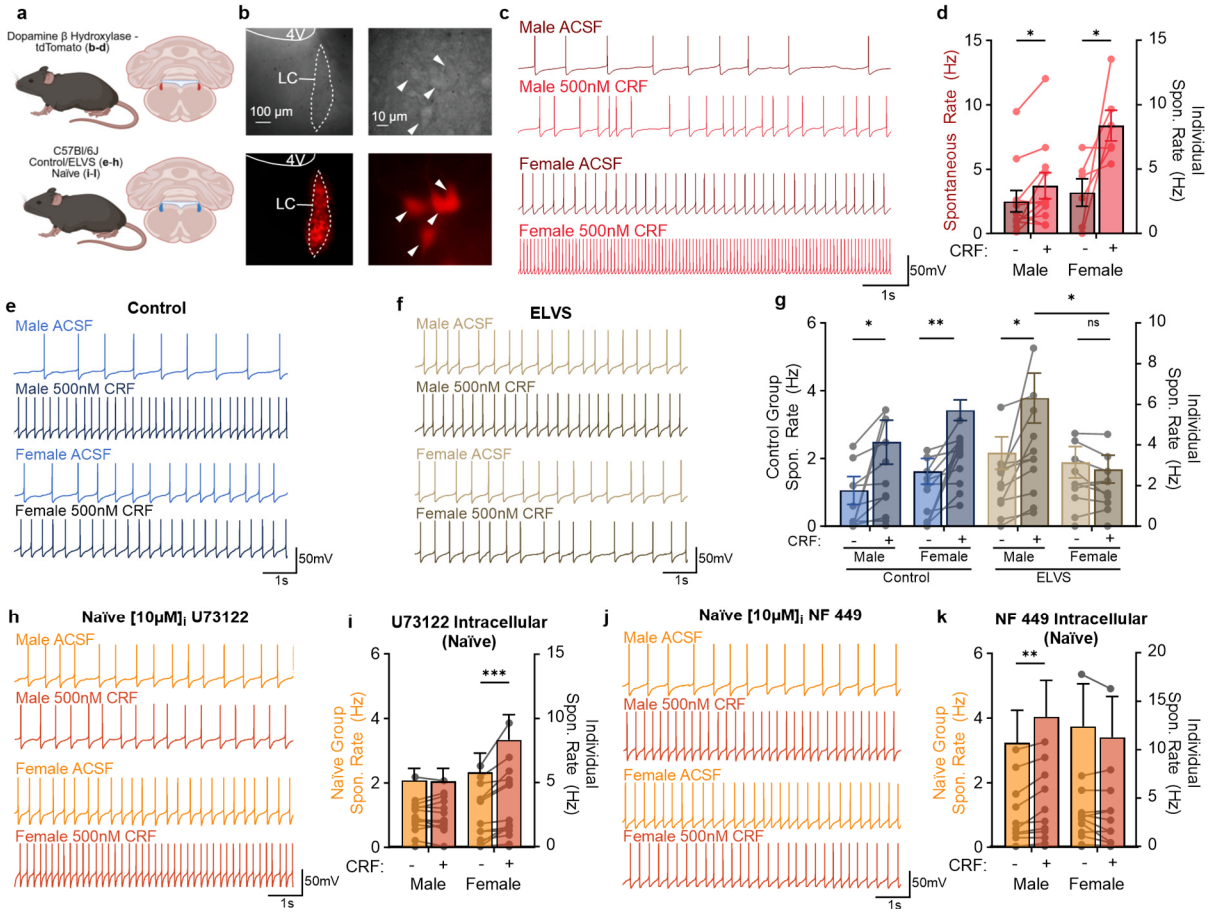

849

850 **Figure 3. CRF excites LC neurons via different pathways in male and female mice and is**
851 **lost in female mice after stress exposure.** (**a**) Schematic of animals used and brain slice
852 approach for recording form LC neurons in mice expressing tdTomato in dopamine β-hydroxylase
853 (DβH)-expressing neurons, control, ELVS-exposed, or naïve mice. (**b**) DIC (top) and fluorescent
854 tdTomato (bottom) image of the LC below the fourth ventricle (left) and a high magnification image
855 of LC neurons in DβH-tdTomato mice. (**c**, **e**, **f**, **h**, **j**) Representative paired membrane voltage
856 traces of spontaneous action potentials generated by LC neurons in ACSF and after bath
857 application of 500nM CRF from DβH-tdTomato (**c**), control C57 (**e**), and ELVS C57 (**f**) mice, or
858 naïve mice with 10µM U73122 (**h**) or 10µM NF 449 (**j**) in the intracellular solution. (**d**, **g**, **i**, **k**)

859 Group spontaneous action potential frequency of LC neurons in ACSF and after bath application
860 of 500nM CRF from DβH-tdTomato (**d**; male: $t(10) = 2.55$, $p = 0.029$; female: $t(5) = 2.61$; $p =$
861 0.048), control and ELVS C57 mice (**g**; Control male – CRF: $p = 0.044$; ELVS male – CRF: $p =$
862 0.0015; Control female – CRF: $p = 0.020$; female control CRF vs. ELVS CRF: $p = 0.045$; ELVS
863 female- CRF: p=0.17), or naïve mice with 10μM U73122 (**i**; male: $W = 3$, $p = 0.93$; female: $W = -$
864 91, $p = 0.0002$) or 10μM NF 449 (**k**; male: $t(10) = 3.44$, $p = 0.0063$; female: $t(12) = 1.53$; $p = 0.15$)
865 in the intracellular solution. In **d**, **g**, **i**, and **k**, the left y-axis corresponds to mean ± SEM group
866 bars and right y-axis corresponds to individual paired values for each individual neuron. All group
867 data are presented as mean ± SEM (bars) for each group, with connected circles representing
868 paired pre- and post-CRF values from individual neurons. Two- (**d**, **i**, **k**) or three-way (**g**)
869 RMANOVAs were used for group comparisons, followed by a paired t-test, Wilcoxon Signed-Rank
870 test for single pairwise comparisons in two-way RMANOVAs or Bonferroni posthoc in three-way
871 RMANOVAs to assess CRF effects. n = 6-11 neurons from N = 2-4 mice (6-8 weeks old) for **c**
872 and **d,** or n = 11-16 neurons from N = 3 mice (5-7 weeks old) for **e**-k. *$p < 0.05$, **$p < 0.01$, ***$p <$
873 0.001 for pairwise comparisons.

874 *Figure 4*

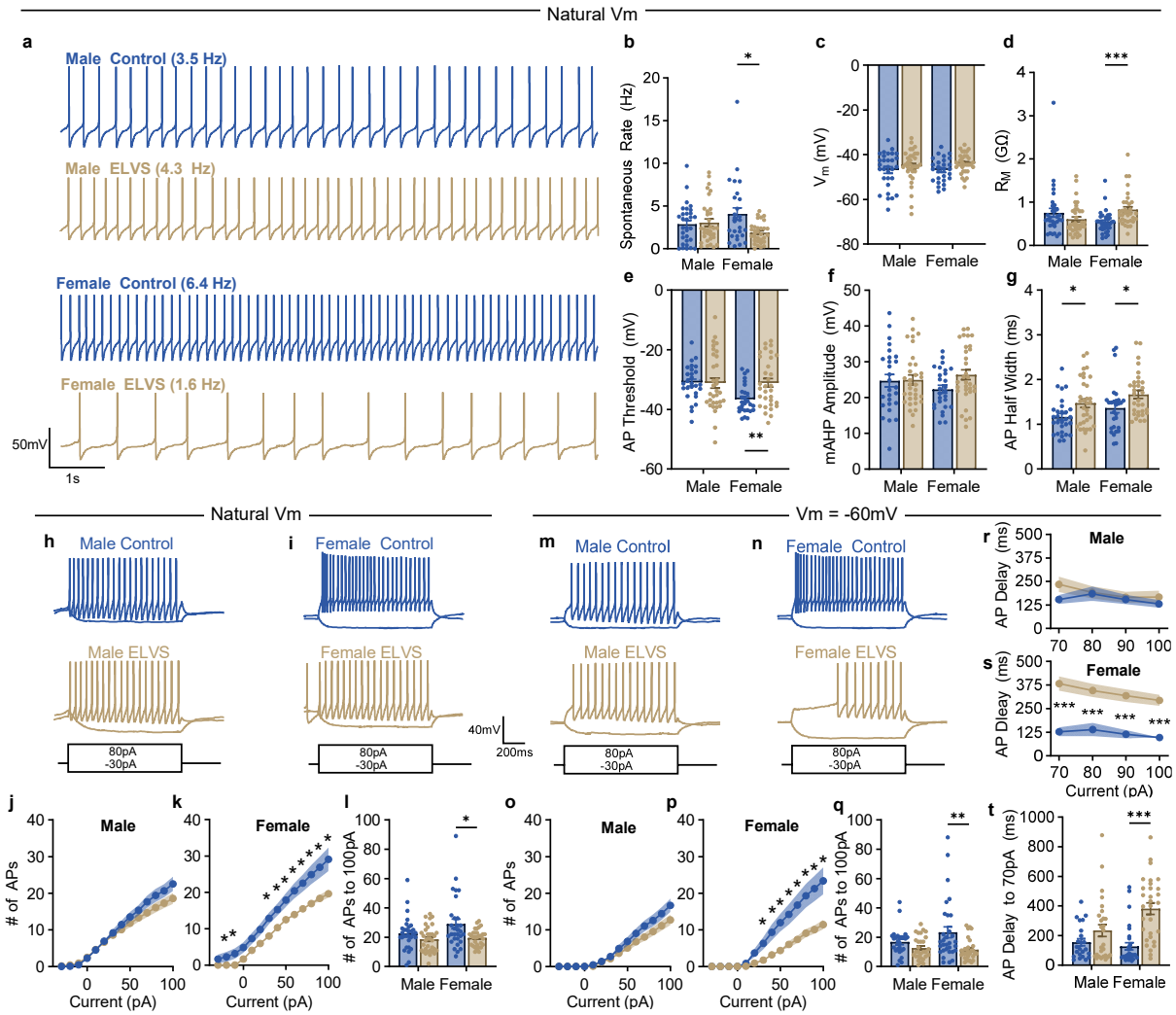

875

876 **Figure 4. ELVS causes reduced LC neuron excitability and increased AP delay time in**

877 **female mice.** (**a, h, i, m, n**) Representative traces of male and female control and ELVS putative

878 LC neurons when firing spontaneously (**a**), in response to +80/-30 pA current injection (1 s) when

879 cells are at their natural resting membrane potential (**h**, **i**) or at -60 mV (**m**, **n**). Note that the same

880 example recordings for both Vm states are provided from the same neuron, some of which are

881 the same in both resting potential states because the natural Vm was at -60 mV. (**b-g**) Action

882 potential spontaneous rate (**b**; males: U = 479.5, *p* = 0.82; females: U = 271.0, p=0.014), resting

883 membrane potential (**c**), membrane resistance (**d**; males: U = 443.0, *p* = 0.14; females: U = 253.5,

884 $p < 0.0001$), action potential (AP) threshold (**e**; males: U = 410.0, $p = 0.61$; females: U = 256.0, p
885 $= 0.0069$), medium after hyperpolarization (mAHP) amplitude (**f**), and AP half-width (**g**; males: U
886 = 314.0, $p = 0.020$; females: U = 295.0, $p = 0.023$) for neurons from each group. (**j**, **k**, **o**, **p**) Number
887 of action potentials elicited by putative LC neurons in response to 1 sec current injection steps
888 from -30 to +100 pA for male (**j**, **o**) and female (**k**, **p**) mice with inter-step membrane potential
889 varying naturally (**j**, **k**; females: U = 293.0 – 370.0, $p = 0.00030 – 0.031$) or maintained near -60
890 mV (**o**, **p**; females: U = 253.0 – 322.0, $p = 0.0019 – 0.038$). (**l, q**) Number of action potentials
891 elicited by putative LC neurons in response to maximum 100 pA for male and female mice with
892 inter-step membrane potential varying naturally (**l**; males: U = 403.5, $p = 0.11$; females: U = 310.0,
893 $p = 0.025$) or maintained near -60 mV (**q**; males: U = 284.0, $p = 0.12$; females: U = 253.0, p =
894 0.0019). (**r**, **s**) Delay time to first action potential after current injection onset present in putative
895 LC neurons in response to 1 sec current injection steps from +70 to +100 pA for male (**r**) and
896 female (**s**; U = 118.0 – 148.5, $p < 0.0001$) mice with inter-step membrane potential maintained
897 near -60 mV. (**t**) Delay time to first action potential after current injection onset present in putative
898 LC neurons in response to 70 pA current injection (1 sec) for male (U = 258.0, $p = 0.31$) and
899 female (U = 124.0, $p < 0.0001$) mice. All group data are presented as mean ± SEM (bars or
900 shading) for each group, with circles representing data from individual neurons. Two- or three-
901 way ANOVAs were used for group comparisons, followed by a t-test or Mann-Whitney U test for
902 single pairwise comparisons to assess stress effects. n = 26-35 neurons from N=4-5 mice (7-8
903 weeks old) for each group. For **b-g**, **l**, **q**, **r-t**, *$p < 0.05$, **$p < 0.01$, ***$p < 0.001$ with two-tailed
904 unpaired t-test or Mann-Whitney U test. For clarity in **j**, **k**, **o**, **p**, only *$p < 0.05$ with Mann-Whitney
905 U test for each current injection.
906
907
908
909

910 *Figure 5*

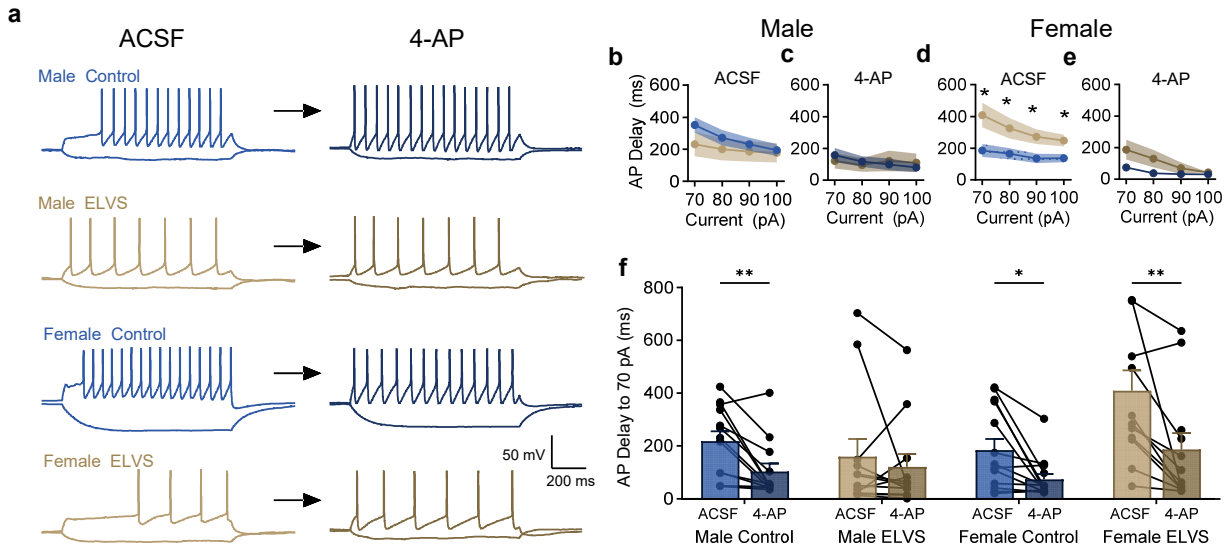

911
912
913 **Figure 5. Blockade of K_A (A-type) potassium channels reduces action potential delay time**
914 **and normalizes ELVS-induced action potential delay time prolongation.** (**a**) Representative
915 recordings from LC neurons in male (top) and female (bottom) control and ELVS mice before (left)
916 and after (right) 5 min bath application of 20 mM 4-aminopyridine (4-AP). **b**-**e**) Delay time to first
917 action potential after current injection onset present in putative LC neurons in response to 1 sec
918 current injection steps from +70 to +100 pA before (**b**, **d**) and after 4-AP application (**c**, **e**) for male
919 (**b**, **c**) and female (**d**,**e**; control: U = 40.0 – 50.0, p = 0.023 – 0.047; ELVS: U = 64.0 - 80.0, p =
920 0.47 – 0.84) control (blue) and ELVS (gold) mice with inter-step membrane potential maintained
921 near -60 mV. (**f**) Delay time to first action potential after current injection onset present in putative
922 LC neurons in response to 70 pA current injection (1 sec) for male (control: W = 80, p = 0.0024;
923 ELVS: W = 24, p = 0.38) and female (control: W = 79, p = 0.010; ELVS: W = 74, p = 0.0015) mice.
924 All group data are presented as mean ± SEM (bars or shading) for each group, with connected
925 circles representing paired data from individual neurons. Three-way ANOVAs and repeated
926 measures ANOVAs were used for group comparisons, followed by a Mann-Whitney U test for
927 single pairwise comparisons to assess stress effects or Wilcoxon Rank-Sum for paired 4-AP

928 effects. n = 11-14 neurons from N=3 mice (7-8 weeks old) for each group. *$p < 0.05$, **$p < 0.01$

929 for each indicated pairwise comparison.

930

Figure 6

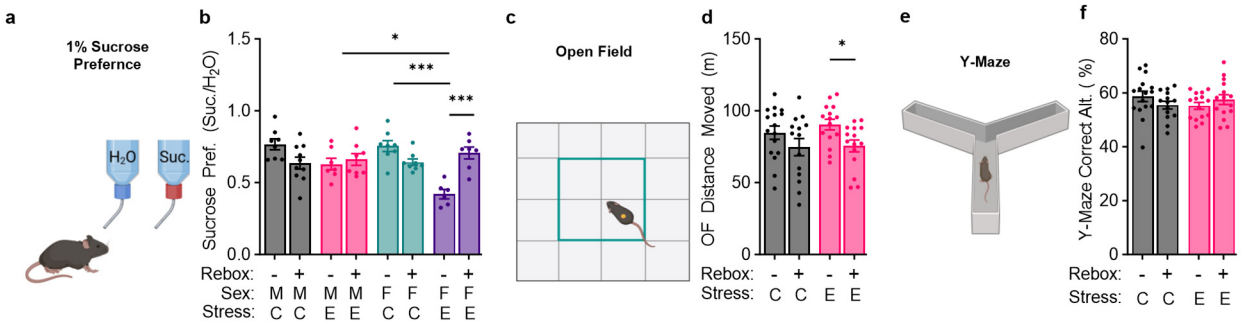

Figure 6. Norepinephrine transporter blockade ameliorates ELVS-induced reduced sucrose preference and increased exploratory activity in female mice. Performance of control and ELVS mice after oral consumption of vehicle (apple juice) or the norepinephrine transporter inhibitor reboxetine (2 mg/kg) in the sucrose preference (**a**, **b**; ELVS female vehicle vs. reboxetine: $p = 0.0001$; Control vs. ELVS female: $p < 0.0001$; ELVS male vs. female: $p = 0.010$), open field (**c**, **d**; control vehicle vs. reboxetine: U = 79.0, $p = 0.18$; ELVS vehicle vs. reboxetine: U = 52.0, $p = 0.011$), or y-maze (**e**, **f**) assays. All group data are presented as mean ± SEM (bars) for each group, with circles representing data from individual mice. Three- or two-way ANOVAs were used for group comparisons, followed by a Bonferroni posthoc or Mann-Whitney U test for pairwise comparisons to assess effects of oral reboxetine treatment on group performance. N = 6-10 mice (7-9 weeks old) for each group and sex. *$p < 0.05$, ***$p < 0.001$ for pairwise comparisons.